

The significance of incorporating a 3-D point source in the inverse scattering series internal multiple attenuator for a 1-D subsurface

Xinglu Lin* and Arthur B. Weglein, M-OSRP/Physics Dept./University of Houston

SUMMARY

In this paper, the 3-D inverse scattering series (ISS) internal multiple attenuation algorithm (Araújo et al., 1994; Weglein et al., 1997, 2003) is modified for a one-dimensional subsurface to incorporate a 3-D point source in multiple predictions, for improved realism and effectiveness. The new algorithm, which assumes the earth is only varying in the z-direction (1-D subsurface/earth, reasonable in many circumstances in Central North sea (Duquet et al., 2013), on-shore Canada, and the Middle East), represents more than a small increase in effectiveness of predicting the shape and amplitude of multiples, compared to a frequently employed 1.5-D ISS internal multiple attenuator (assuming a 2-D line source and a 1-D earth). The numerical tests are performed on a 3-D source synthetic data set from a 1-D subsurface. The results demonstrate that the new algorithm incorporating a 3-D point source can change the prediction from 'causing harm' to 'providing benefit' in comparison to an internal multiple attenuation algorithm that assumes a 1-D earth and a line source.

INTRODUCTION

The current state of ISS algorithms provides a multidimensional procedure that eliminates all free-surface multiples and attenuates all internal multiples (Carvalho, 1992; Araújo et al., 1994; Weglein et al., 1997, 2003). Yanglei Zou and Chao Ma are pioneering new ISS capability for internal multiple removal (Zou and Weglein, 2014; Liang et al., 2013; Ma and Weglein, 2014). This approach has its unique strengths in that it does not require subsurface information and is even independent of the earth model-type. These multidimensional methods, the ISS internal multiple attenuation algorithm (Araújo et al., 1994; Weglein et al., 1997) can predict the accurate time and approximate amplitude of internal multiple (that are generated by the reflectors below the free-surface). The data requirement of this method depends on how many dimensions are assumed to be spatially variable in the subsurface. For example, the original 2-D ISS internal multiple attenuation algorithm (assuming 2-D line sources and 2-D line receivers) requires a collection of shot records on a line. However, for a 3-D subsurface (assuming 3-D point sources and 3-D point receivers), the algorithm needs the sources everywhere on the measurement plane and each source needs the receivers everywhere on the plane.

The implementations on this method have shown promising results for marine (e.g. Ferreira, 2011; Matson and Weglein, 1996) and on-shore cases (e.g. Fu et al., 2010; Luo et al., 2011; Terenghi et al., 2011). There are circumstances where it is reasonable to assume a 1-D subsurface (e.g. Central North sea (Duquet et al., 2013), on-shore Canada, and the Middle East). Recently, the 1.5-D ISS internal multiple attenuator (the algorithm reduced from a complete 2-D ISS internal multiple atten-

uation algorithm for a 1-D subsurface) has been successfully applied on Saudi Aramco on-shore data (Luo et al., 2011) and also produced a positive result for the Encana land data (Fu and Weglein, 2014).

In this abstract, we will incorporate a 3-D point source into the 1-D subsurface ISS internal multiple attenuation algorithm to develop a more realistic algorithm and to evaluate the significance of including the 3-D source in the algorithm.

THE 3-D AND 2-D ISS INTERNAL MULTIPLE ATTENUATION ALGORITHM

The ISS internal multiple attenuator was originally proposed by Araújo et al. (1994) and Weglein et al. (1997). The preparation of the 3-D ISS internal multiple prediction starts from data $D(x_g, y_g, \epsilon_g, x_s, y_s, \epsilon_s, t)$, where (x_g, y_g, ϵ_g) and (x_s, y_s, ϵ_s) are the receiver- and source-location, respectively. For the fixed depth of sources and receivers (omit ϵ_s, ϵ_g), the b_1 term is defined by the data in wavenumber-frequency domain as $b_1(\vec{k}_g, \vec{k}_s, q_g + q_s) = -2iq_s \cdot D(\vec{k}_g, \vec{k}_s, \omega)$, where the vertical wavenumber is $q_i = \text{sgn}(\omega) \sqrt{(\omega/c_0)^2 - k_{x_i}^2 - k_{y_i}^2}$, $i \in \{g, s\}$ and $\vec{k}_g = (k_{x_g}, k_{y_g})$, $\vec{k}_s = (k_{x_s}, k_{y_s})$. The b_1 term can be Fourier transformed to the depth domain as $b_1(\vec{k}_g, \vec{k}_s, z)$, and corresponds to an un-collapsed Stolt migration. The ISS internal multiple attenuation algorithm in 3-D is

$$\begin{aligned}
 & b_3^{3D}(k_{x_g}, k_{y_g}, k_{x_s}, k_{y_s}; \omega) \\
 &= \frac{1}{(2\pi)^4} \iint dk_{x_1} dk_{x_2} \iint dk_{y_1} dk_{y_2} e^{-iq_1(\epsilon_g - \epsilon_s)} e^{iq_2(\epsilon_g - \epsilon_s)} \\
 & \quad \times \int_{-\infty}^{+\infty} dz_1 b_1(k_{x_g}, k_{y_g}, k_{x_1}, k_{y_1}, z_1) e^{i(q_g + q_1)z_1} \\
 & \quad \times \int_{-\infty}^{z_1 - \epsilon} dz_2 b_1(k_{x_1}, k_{y_1}, k_{x_2}, k_{y_2}, z_2) e^{-i(q_1 + q_2)z_2} \\
 & \quad \times \int_{z_2 + \epsilon}^{+\infty} dz_3 b_1(k_{x_2}, k_{y_2}, k_{x_s}, k_{y_s}, z_3) e^{i(q_2 + q_s)z_3}, \quad (1)
 \end{aligned}$$

where the $q_i = \text{sgn}(\omega) \sqrt{(\omega/c_0)^2 - k_{x_i}^2 - k_{y_i}^2}$, $i \in \{g, 1, 2, s\}$, and $b_3^{3D}(k_{x_g}, k_{y_g}, k_{x_s}, k_{y_s}, \omega)$ is a 3-D internal multiple attenuator in wavenumber-frequency domain. The 3-D algorithm in equation (1) assumes that the acquisition applies 3-D sources and 3-D receivers for a 3-D subsurface. Two dimension space and time inverse Fourier transforming $b_3^{3D}(k_{x_g}, k_{y_g}, k_{x_s}, k_{y_s}, \omega) / (-2iq_s)$ can produce the 3-D space-time attenuator, which predict the internal multiple accurately in time and approximately in amplitude. In addition, $(b_1 + b_3) / (-2iq_s)$ can generate the result after multiple removal when it is returned to the space-time domain.

Similarly, a set of 2-D data $D(x_g, x_s, t)$ can be transformed into wavenumber-frequency domain as $D(k_g, k_s, \omega)$, which defines

Incorporating a 3-D point source in the ISS internal multiple attenuator for a 1-D subsurface

the 2-D $b_1(k_g, k_s, q_g + q_s) = -2iq_s \cdot D(k_g, k_s, \omega)$. And then the 2-D ISS internal multiple attenuation algorithm is

$$\begin{aligned} & b_3^{2D}(k_g, k_s; \omega) \\ &= \frac{1}{(2\pi)^2} \iint dk_1 dk_2 e^{-iq_1(\varepsilon_g - \varepsilon_s)} e^{iq_2(\varepsilon_g - \varepsilon_s)} \\ & \times \int_{-\infty}^{+\infty} dz_1 b_1(k_g, k_1, z_1) e^{i(q_s + q_1)z_1} \\ & \times \int_{-\infty}^{z_1 - \varepsilon} dz_2 b_1(k_1, k_2, z_2) e^{-i(q_1 + q_2)z_2} \\ & \times \int_{z_2 + \varepsilon}^{+\infty} dz_3 b_1(k_2, k_s, z_2) e^{i(q_2 + q_s)z_3}, \end{aligned} \quad (2)$$

where the vertical wavenumber is $q_i = \text{sgn}(\omega) \sqrt{(\omega/c_0)^2 - k_i^2}$, $i \in \{g, 1, 2, s\}$, $b_1(k_g, k_s, z)$ is an un-collapsed Stolt migration of a 2-D data (transform $b_1(k_g, k_s, q_g + q_s)$ back to depth domain), and $b_3^{2D}(k_g, k_s, \omega)$ is a 2-D internal multiple attenuator in wavenumber-frequency domain. The 2-D attenuator in space-time domain can be obtained by inverse Fourier transforming $b_3^{2D}(k_g, k_s, \omega)/(-2iq_s)$. In contrast to the 3-D case, algorithm in equation (2) assumes a 2-D subsurface, in which the acquisition corresponds to 2-D line sources and 2-D line receivers.

In the following sections, both the 3-D algorithm and 2-D algorithm are reduced for the data from a 1-D subsurface, where in the 3-D case the source is a 3-D point source and in the 2-D case the source is a line source. For convenience, the superscript *1DE* represents the 1-D earth assumption for different sources (For example, 2-D line source 1-D earth: *2D1DE*; 3-D point source 1-D earth: *3D1DE*).

THE ISS INTERNAL MULTIPLE ATTENUATOR ASSUMING A 2-D LINE SOURCE FOR A 1-D SUBSURFACE

In developing the algorithm for a 1-D earth pre-stack data, it was natural that people started with the 2-D ISS internal multiple attenuation algorithm and then reduced it for a 1-D subsurface data. The data that occurs in the 2-D earth can be presented as $D(x_g, x_s, \omega)$ or $D(x_m, x_h, \omega)$ in space-frequency domain, where $x_m = x_g + x_s$ and $x_h = x_g - x_s$. The data from a 1-D earth, shown as $D^{2D1DE}(x_h, \omega)$, only depends on the source-receiver offset (x_h) and the frequency (ω). The Fourier transform over the 2-D data for a 1-D earth, which is needed for the algorithm, can be shown as,

$$\begin{aligned} D(k_g, k_s; \omega) &= \iint e^{ik_g x_g} e^{-ik_s x_s} D^{2D1DE}(x_h, \omega) dx_g dx_s \\ &= \frac{1}{2} \int e^{ik_h x_h} D^{2D1DE}(x_h, \omega) dx_h \int e^{ik_m x_m} dx_m \\ &= D^{2D1DE}(k_h, \omega) (2\pi) \cdot \delta(k_g - k_s), \end{aligned} \quad (3)$$

where $k_h = \frac{k_g + k_s}{2}$ and $k_m = \frac{k_g - k_s}{2}$. The data is independent of x_m and can come out of the integral. Consequently, the Fourier transform integral over x_m can produce a Dirac delta function in k_m . b_1 is defined as $b_1(k_g, k_s, q_g + q_s) = -2iq_s \cdot$

$D(k_g, k_s, \omega)$. The un-collapsed Stolt migration b_1 can be expressed by b_1^{2D1DE} as,

$$b_1(k_g, k_s, z) = b_1^{2D1DE}(k_h, z) (2\pi) \cdot \delta(k_g - k_s). \quad (4)$$

By applying this 1-D earth b_1 to the equation (2), the lateral integrals ($\int \int dk_1 dk_2$) can be evaluated by the Dirac delta functions. Then equation (2) produces the reduced 1.5-D internal multiple attenuator as,

$$\begin{aligned} & b_3^{2D1DE}(k_h; \omega) = \\ & \int_{-\infty}^{+\infty} dz_1 b_1^{2D1DE}(k_h, z_1) e^{i2qz_1} \int_{-\infty}^{z_1 - \varepsilon} dz_2 b_1^{2D1DE}(k_h, z_2) e^{-i2qz_2} \\ & \times \int_{z_2 + \varepsilon}^{+\infty} dz_3 b_1^{2D1DE}(k_h, z_3) e^{i2qz_3}, \end{aligned} \quad (5)$$

where $k_h = k_g = k_s$ (evaluating by the Dirac delta functions) and $q = \text{sgn}(\omega) \sqrt{(\omega/c_0)^2 - k_h^2}$. Prediction D_3 in the space domain can be obtained by an inverse Fourier transform as,

$$D_3^{2D1DE}(x_h; \omega) = \frac{1}{2\pi} \int b_3^{2D1DE}(k_h; \omega) / (-2iq_s) e^{ik_h x_h} dk_h. \quad (6)$$

The process following equations (5) and then (6) gives us the ISS internal multiple attenuation algorithm assuming a 2-D line source for a 1-D subsurface.

THE ISS INTERNAL MULTIPLE ATTENUATOR ASSUMING A 3-D POINT SOURCE FOR A 1-D SUBSURFACE

The 3-D data generated by a 1-D earth only depends on the source-receiver offset and the frequency, which has a spatial circular symmetry in cylindrical coordinates (independence of azimuth angle). This symmetry makes it convenient to study the 1-D earth problem with cylindrical coordinates. The 3-D vectors (x, y, z) and (k_x, k_y, k_z) in Cartesian coordinates can be transformed to (r_i, θ_i, z_i) and (k_{ri}, ϕ_i, k_{zi}) , $i \in \{g, 1, 2, s\}$, in cylindrical coordinates, which is characterized by a radial length, an azimuth angle and a vertical position. The dependence of a 3-D data for a 1-D earth can be expressed as $D^{3D1DE}(|\vec{r}_g - \vec{r}_s|, \omega)$ or $D^{3D1DE}(r_h, \omega)$, where the \vec{r}_g and \vec{r}_s are the projection of receiver and source locations on x-y plane, respectively. r_h is the magnitude of the difference between \vec{r}_g and \vec{r}_s . Due to the cylindrical symmetry, the 3-D source-1-D subsurface data can be transformed to (k_{ri}, ω) domain as,

$$D(\vec{k}_g, \vec{k}_s; \omega) = D^{3D1DE}(k_{rh}; \omega) (2\pi)^2 \frac{\delta(k_{rg} - k_{rs}) \delta(\phi_g - \phi_s)}{k_{rg}}, \quad (7)$$

where $k_{rh} = k_{rg}$. The receivers are required along the r-direction as $D^{3D1DE}(r_h, \omega)$, because

$$D^{3D1DE}(k_{rh}; \omega) = 2\pi \int_0^{\infty} D^{3D1DE}(r_h; \omega) J_0(k_{rh} r_h) r_h dr_h. \quad (8)$$

The form of data in $(k_{ri}; \omega)$ domain (equation (7)) contains the Dirac delta functions in cylindrical coordinates, which is equivalent to $\delta(k_{xg} - k_{xs}) \delta(k_{yg} - k_{ys})$ in Cartesian coordinates. Similar to the 2-D case, b_1 back to depth domain is,

$$b_1(\vec{k}_g, \vec{k}_s, z) = b_1^{3D1DE}(k_{rg}, z) (2\pi)^2 \frac{\delta(k_{rg} - k_{rs}) \delta(\phi_g - \phi_s)}{k_{rg}}, \quad (9)$$

Incorporating a 3-D point source in the ISS internal multiple attenuator for a 1-D subsurface

which is a 3-D un-collapsed Stolt migration. Substitute this term into the full 3-D ISS internal multiple attenuation algorithm in equation (1) with arranging the integral variable from $dk_x dk_y$ to $k_r dk_r d\phi$. The lateral integrals $\iiint k_{r1} dk_{r1} d\phi_1$ $k_{r2} dk_{r2} d\phi_2$ can be evaluated due to the Dirac delta functions, as above. The reduced form of the 3-D algorithm is

$$b_3^{3D1DE}(k_{rh}; \omega) = \int_{-\infty}^{+\infty} dz_1 b_1^{3D1DE}(k_{rh}, z_1) e^{i2qz_1} \int_{-\infty}^{z_1-\varepsilon} dz_2 b_1^{3D1DE}(k_{rh}, z_2) e^{-i2qz_2} \times \int_{z_2+\varepsilon}^{+\infty} dz_3 b_1^{3D1DE}(k_{rh}, z_3) e^{i2qz_3}, \quad (10)$$

where $k_{rh} = k_{rg} = k_{rs}$ (evaluated by Dirac delta functions), vertical wavenumber $q = \text{sgn}(\omega) \sqrt{(\omega/c_0)^2 - k_{rh}^2}$ and $\varepsilon_g = \varepsilon_s$ (receivers and sources are located at the same depth). Equation (10) has the same form as the reduced 2-D internal multiple attenuator (equation (5)) for 1-D subsurface in wavenumber-frequency domain.

$b_3^{3D1DE}(k_{rh}; \omega)$ needs to be transformed back to the space domain by an inverse Hankel transform (derived from two dimension Fourier transform due to the independence of the azimuth angle), instead of an inverse Fourier transform. The internal multiple prediction $D_3^{3D1DE}(r_h; \omega)$ can be obtained by using,

$$D_3^{3D1DE}(r_h; \omega) = \frac{1}{2\pi} \int_0^{\infty} J_0(k_{rh} \cdot r_h) \frac{b_3^{3D1DE}(k_{rh}; \omega)}{-2iq_s} k_{rh} dk_{rh}. \quad (11)$$

We can rewrite the integral above using Bessel functions of the third kind (Hankel function) H_0^+ as,

$$D_3^{3D1DE}(r_h; \omega) = \frac{1}{4\pi} \int_{-\infty}^{+\infty} H_0^+(k_{rh} \cdot r_h) \frac{b_3^{3D1DE}(k_{rh}; \omega)}{-2iq_s} k_{rh} dk_{rh}, \quad (12)$$

where $q = \text{sgn}(\omega) \sqrt{(\omega/c_0)^2 - k_{rh}^2}$. Considering the high computational costs in this transform, we can use the approximate asymptotic Hankel function to improve the efficiency. Then the asymptotic Hankel transform is,

$$D_3^{3D1DE}(r_h; \omega) = \frac{1}{2\pi} \int_{-\infty}^{+\infty} \sqrt{\frac{k_{rh}}{i2\pi r_h}} \frac{b_3^{3D1DE}(k_{rh}; \omega)}{-2iq_s} e^{ik_{rh} r_h} dk_{rh}. \quad (13)$$

In a specified acquisition geometry that sources and receivers are on the same streamer in 3-D survey, we can make r along any angle in x-y plane, including $r = x$. The equation (10) combining with equation (11) or (13) form the ISS internal multiple attenuator assuming a 3-D point source for 1-D subsurface.

NUMERICAL RESULTS

The synthetic 3-D source data are generated based on a 1-D acoustic layered model in Figure 1 using a broad bandwidth. Since the data set is generated in (k_{rh}, q) domain by reflectivity method, we assume that the data is transformed from space-time domain to wavenumber-frequency domain by space Fourier-Bessel transform (Hankel transform) and time

Fourier transform. The dataset is one pre-stack shot record (see Figure 2 (a)) without free-surface multiple or ghost, which satisfies the data requirements of both the ISS internal multiple attenuation algorithm assuming a 2-D line source (equation (5),(6)) and a 3-D point source (equation (10), (11) or (13)).

The comparisons between the original data, the 2-D line source prediction and the 3-D point source predictions are shown in four shot gather plots (see Figure 2). The original 3-D source data from a 1-D earth is shown in Figure 2 (a), which contains two primaries and one internal multiple events. Figure 2 (c) presents the internal multiple prediction assuming a 2-D line source, in which the tail spread (a non-spherical wave) is due to the impulse signature in a 2-D Green's function. Both Figure 2 (b) and (d) provides the predictions assuming a 3-D point source. The difference is that the result in (d) employs an asymptotic Bessel function (equation (13)) in order to transform the prediction back to space domain, instead of doing a Hankel transform (equation (11)) in the prediction shown in (b). The reason is because the efficiency of a 3-D point source prediction is the same as a 2-D line source prediction when an asymptotic Bessel function is used.

All the predictions here produce an accurate time of the internal multiple, but different wavelet shape (Figure 2 (c)) or amplitude (Figure 2 (b) (c) (d)) from the original internal multiple. In a further step, we explore the effectiveness of different predictions by comparing results in near-offset (Figure 3 (a) (b), trace 2) and far-offset (Figure 3 (c) (d), trace 60).

Figure 3 (a) and (c) demonstrate that the 2-D line source prediction (blue line) can generate a deviated wavelet and a much larger amplitude than original internal multiple (red line). In this case, direct subtracting the prediction from the data can produce a larger multiple event in the de-multiple result, which is harmful to the subsequent processing. Meanwhile, the 3-D source predictions (black line, green line) always will be an attenuator as expected, for both near- and far- offset (smaller amplitude compared to original internal multiple (red line)).

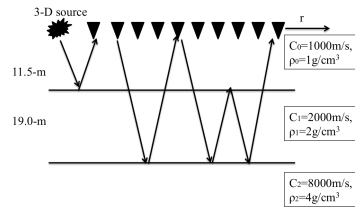


Figure 1: Acoustic model used to generate synthetic 3-D point source data.

Figure 3 (b) and (d) presents the difference between the original data (red line) and the 3-D source predictions on near- and far-offset traces, respectively. The wiggle plots (corresponding to the time slot in red box in Figure 3 (a) and (c)) are shown in a larger scale. The results demonstrate that the predictions assuming a 3-D source are always attenuators, which is the characteristic of the ISS internal multiple attenuation algorithm. For a near-offset trace (see Figure 3 (b)), the prediction using an asymptotic Bessel (green line), which is a far-field approximation, is not as effective as the prediction retaining Hankel

Incorporating a 3-D point source in the ISS internal multiple attenuator for a 1-D subsurface

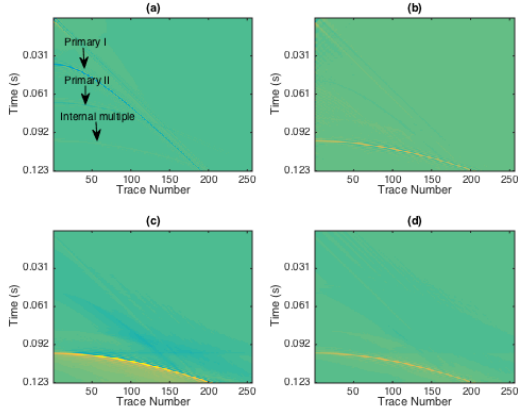


Figure 2: (a) One shot gather of a 3-D source-1-D earth data; (b) ISS internal multiple prediction assuming a 3-D point source; (c) ISS internal multiple prediction assuming a 2-D line source; (d) ISS internal multiple prediction assuming a 3-D point source using an asymptotic Bessel function.

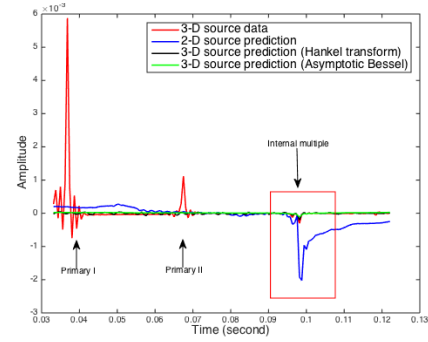
transform in it (**black** line). Nevertheless, for the far-offset trace (see Figure 3 (d)) the amplitudes of these two predictions tend to be the same. Please notice that when the asymptotic Bessel function is applied to a 3-D point source attenuator for 1-D subsurface, the computational cost of it can be reduced to the same as the cost of a 1.5-D line source attenuator, which can finish its prediction in the order of seconds for this small size experimental data.

CONCLUSION

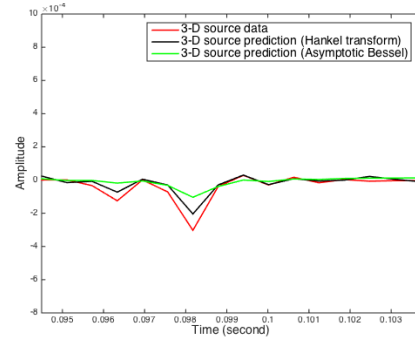
In this paper, a reduced and modified 3-D source ISS internal multiple attenuator has been proposed for a 1-D subsurface, which enhances the effectiveness of predicting the shape and amplitude of the internal multiples. Numerical tests and analysis illustrate that with the data generated by a 3-D point source it is important to incorporate that source dimension in the ISS internal multiple attenuation algorithm. That incorporation will always reduce the internal multiple. Using an internal multiple predictor that assumes a 2-D line source on data from a 3-D point source can make the multiple larger amplitude. Therefore, it is essential to incorporate a 3-D point source in internal multiple algorithms when the subsurface is 1-D, 2-D or 3-D. Ignoring the 3-D source inclusion on real data can result in an effective and useful algorithm making the multiple problem worse. That was an interesting and surprising result for the important role that a 3-D source accommodation is for internal multiple prediction effectiveness.

ACKNOWLEDGMENTS

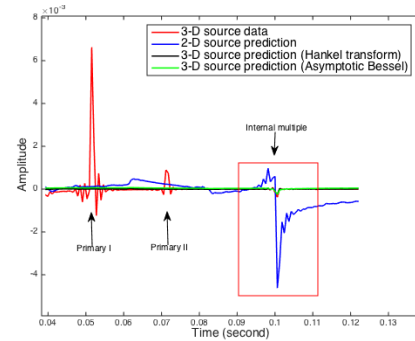
We are grateful to all the M-OSRP sponsors for their long-term support and encouragements.



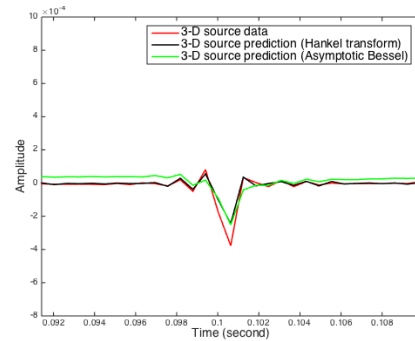
(a) Wiggle comparison of trace 2



(b) Plot the slot in the red box in (a) without the 2-D source prediction in a larger scale



(c) Wiggle comparison of trace 60



(d) Plot the slot in the red box in (c) without the 2-D source prediction in a larger scale

Figure 3: Wiggle comparison of trace 2 (a) (b) and trace 60 (c) (d); **Red** line: original 3-D source-1-D earth data; **Blue** line: ISS internal multiple prediction assuming a 2-D line source; **Black** line: ISS internal multiple prediction assuming a 3-D point source; **Green** line: ISS internal multiple prediction assuming a 3-D point source using an asymptotic Bessel function.

Incorporating a 3-D point source in the ISS internal multiple attenuator for a 1-D subsurface

REFERENCES

- Araújo, F. V., A. Weglein, P. M. Carvalho, and R. Stolt, 1994, Inverse scattering series for multiple attenuation: An example with surface and internal multiples: 64th Annual International Meeting, SEG, Expanded Abstracts, 1039–1041.
- Carvalho, P. M., 1992, Free-surface multiple reflection elimination method based on nonlinear inversion of seismic data: PhD thesis, Universidade Federal da Bahia.
- Duquet, B., A. Chavanne, P. Poupion, M. Rowlands, B. Santos-Luis, and J. M. Ugolini, 2013, Seismic processing and imaging in central north sea area - recents advances and remaining challenges: 75th EAGE conference.
- Ferreira, A., 2011, Internal multiple removal in offshore offshore brazil seismic data using the inverse scattering series: Master Thesis, University of Houston.
- Fu, Q., Y. Luo, P. G. Kelamis, G. Huo, G. Sindi, S.-Y. Hsu, and A. B. Weglein, 2010, The inverse scattering series approach towards the elimination of land internal multiples: 80th Annual International Meeting, SEG, Expanded Abstracts, 3456–3461.
- Fu, Q., and A. B. Weglein, 2014, Internal multiple attenuation on encana data: 84th Annual International Meeting, SEG, Expanded Abstracts, 4118–4123.
- Liang, H., C. Ma, and A. B. Weglein, 2013, General theory for accommodating primaries and multiples in internal multiple algorithm: Analysis and numerical tests: 83th Annual International Meeting, SEG, Expanded Abstracts, 4178–4183.
- Luo, Y., P. G. Kelamis, Q. Fu, G. Huo, G. Sindi, S.-Y. Hsu, and A. B. Weglein, 2011, Elimination of land internal multiple based on the inverse scattering series: *The Leading Edge*, **30**, 884–889.
- Ma, C., and A. B. Weglein, 2014, Including higher-order inverse scattering series terms to address a serious shortcoming/problem of the internal-multiple attenuator: Exemplifying the problem and its resolution: 84th Annual International Meeting, SEG, Expanded Abstracts, 4124–4129.
- Matson, K., and A. B. Weglein, 1996, Removal of elastic interface multiples from land and ocean bottom data using inverse scattering: 66th Annual International Meeting, SEG, Expanded Abstracts., 1526–1529.
- Terenghi, P., S.-Y. Hsu, A. B. Weglein, and X. Li, 2011, Exemplifying the specific properties of the inverse scattering series internal-multiple attenuation method that reside behind its capability for complex onshore and marine multiples: *The Leading Edge*, **30**, 876–882.
- Weglein, A. B., F. V. Araújo, P. M. Carvalho, R. H. Stolt, K. H. Matson, R. T. Coates, D. Corrigan, D. J. Foster, S. A. Shaw, and H. Zhang, 2003, Inverse scattering series and seismic exploration: *Inverse Problems*, R27–R83.
- Weglein, A. B., F. A. Gasparotto, P. M. Carvalho, and R. H. Stolt, 1997, An inverse-scattering series method for attenuating multiples in seismic reflection data: *Geophysics*, **62**, 1975–1989.
- Zou, Y., and A. B. Weglein, 2014, An internal-multiple elimination algorithm for all reflectors for 1d algorithm, part 1: Strengths and limitations: *Journal of seismic exploration*, **23**, 393–404.